Colloids and Surfaces A 606 (2020) 125384

Contents lists available at ScienceDirect

Colloids and Surfaces A

journal homepage: www.elsevier.com/locate/colsurfa

Single and ensemble response of colloidal ellipsoids to a nearby *ac* electrode

Jiarui Yan[a], Aidin Rashidi[a], Christopher L. Wirth[b,*]

[a] Department of Chemical and Biomedical Engineering, Washkewicz College of Engineering, Cleveland State University, 2121 Euclid Avenue, Cleveland, OH, 44115, United States

[b] Department of Chemical and Biomolecular Engineering, Case School of Engineering, Case Western Reserve University, Cleveland, OH, 44106, United States

GRAPHICAL ABSTRACT

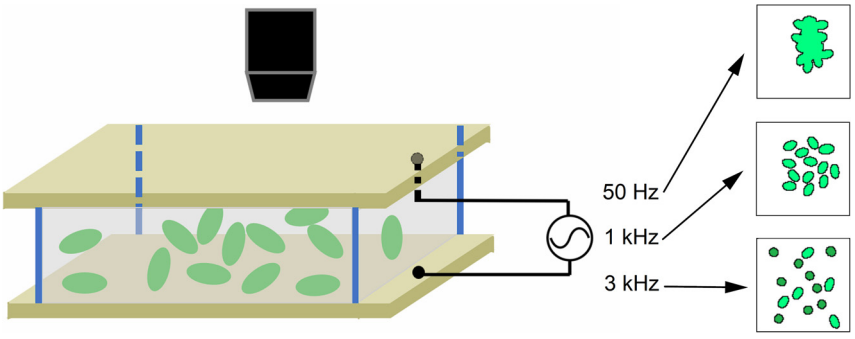

ARTICLE INFO

Keywords:
Electrokinetics
Colloidal assembly
Anisotropic particles

ABSTRACT

Anisotropic colloids can be used as building blocks for fabricating assemblies with complex microstructure and function. External electric fields are one key tool used to assemble such colloidal structures. Herein, we utilized a parallel plate electrode geometry to drive motion of micrometer scale ellipsoidal colloids. The response of pseudo 2D layers of ellipsoids with systematically altered aspect ratios was measured as a function of electric field strength and frequency. We found there to be a weak dependence of ellipsoid ensemble structure on aspect ratio. Namely, regions of aggregation and separation were only slightly dependent on particle aspect ratio. We found that ellipsoids with a smaller aspect ratio tended to align with the electric field, while high aspect ratio ellipsoids did not in response to an electric field of the magnitude and time scale used herein. In addition, we found the kinetics of aggregation of colloids to be very similar regardless of aspect ratio. Complementary experiments utilizing these data demonstrated long-lasting deposition of ellipsoids in energetically unfavorable orientations, which is being used as a model system for the measurement of light scattered from an evanescent wave by an ellipsoid.

1. Introduction

The response of colloidal particles to an external field has been investigated as a route for fabricating optical materials that interact with light in technologically useful ways [1–3]. One such fabrication method uses a parallel plate electrode geometry to drive assembly of a pseudo 2D layer of colloidal particles near, but not adhered, to a polarized electrode [4]. Extensive work in this area has been completed by multiple groups on the response of colloidal spheres to steady and oscillatory electric fields [5–20]. These studies found that particles

* Corresponding author.
E-mail address: wirth@case.edu (C.L. Wirth).

https://doi.org/10.1016/j.colsurfa.2020.125384
Received 11 June 2020; Received in revised form 10 July 2020; Accepted 31 July 2020
Available online 05 August 2020

respond to electrically driven flows along the particle and electrode surfaces to induce net attractive or repulsive interactions between particles. Colloidal arrays are quickly formed from the dynamic response of these particles to those hydrodynamic interactions mediated by electrokinetic flows. Work in this area focused on isotropic particles for nearly two decades, but recent experiments with this electrode geometry and others demonstrated the profound difference in how individual and ensembles of anisotropic particles respond to the nearby electrode [21–29].

Motivation for work on the response of anisotropic particles to an electric field resides on multiple fronts. The first is that colloidal particles with anisotropy in shape or surface chemistry have the potential to form colloidal assemblies with a more sophisticated structure as compared to those fabricated from colloidal spheres [30]. Isotropic colloidal spheres form assemblies via isotropic interactions that typically restrict structures to hexagonal arrays with interparticle spacing ranging from close-packed to a few particle diameters. However, anisotropic particles will interact via spatially anisotropic forces that will induce assemblies with more complexity. Structurally complex assemblies with internal directionality have greater potential for interacting with light as compared to hexagonal arrays. The second motivation for this work is to drive the directed motion of individual anisotropic particles, which offer more control over locomotion and trajectories as compared to isotropic particles [25,31–33]. Colloidal particles with anisotropy in shape and surface chemistry display motility in response to externally applied electric fields. For instance, a doublet of unequal lobe size will propel in an oscillatory electric field in the direction of either the small or large lobe, depending on the combination of particle and electric field conditions [25]. The origin of this motion is in the mismatch of electrokinetic flows that arise on either the particle or electrode surface, which then induces a mismatch in local force that propels the particle. Finally, our group is specifically interested in the external control of the orientation of non-spherical particles in energetically unfavorable positions. This interest arises from the need to collect the light scattered from an evanescent wave by a non-spherical particle for the development of Scattering Morphology Resolved TIRM [34]. Given that particles described herein are typically < 300 nm in separation distance from the nearby electrode, an evanescent wave with decay length of $\sim$100 nm would readily interact with these particles thereby scattering light.

Herein, we summarize experimental results for the response of colloidal ellipsoids to a nearby electrode undergoing *ac* polarization. Polystyrene ellipsoids of varying aspect ratio were first fabricated via film stretching and then were suspended in low concentration electrolyte. The response of ellipsoids that had formed a quasi-2D layer near an electrode polarized at low-frequency electric fields was measured at intermediate concentration. Both the ensemble structure and aggregation kinetics was measured. First, we found that ellipsoids responded to the electric field by either aggregating or separating depending on the electric field conditions. Further, we found that ellipsoids oriented parallel to the electric field at certain conditions. We then modulated the electric field to achieve long-lasting deposition of ellipsoids at this orientation. Finally, we found the rate constant for aggregation did not depend on particle shape for the aspect ratios measured herein. Although our work shows some differences in the way that ellipsoids respond to an electric field as compared to spheres, the overall aggregation behavior was similar. This suggests that work conducted for spheres over the last two decades is applicable to the response of ellipsoids of these aspect ratios to a nearby polarized electrode.

2. Experimental

2.1. Fabrication of ellipsoids

Colloidal ellipsoids were fabricated with an established film-stretching procedure [35]. Briefly, 7.5 g of polyvinyl alcohol (PVA, POVAL 40–88 Kuraray polyvinyl alcohol) was first added slowly to 300 g of ultra-pure water in a clean bottle. Addition of PVA too rapidly will lead to the formation of non-dissolvable clumps. The PVA solution was stirred for 24 h and then filtered with filter paper (Lab Safety Supply, Grade CFP4, 18.5 cm diameter, 25 μm pore size) to remove any remaining non-dissolved PVA. The filtered solution was allowed to rest to minimize bubbles. Next, 1.0 g of nominally 5 μm diameter polystyrene sulfate latex particles (Molecular Probes, lot# 1964358, 4% w/v) was added to the PVA solution. The bottle was then gently swirled to ensure dispersal of the latex without production of bubbles in the PVA solution. The PVA solution was then slowly poured onto a 25 cm × 25 cm square cast constructed on a polyvinylidene difluoride (PVDF) surface. The bubbles were pushed to the edges with a clean spatula. The casted film was left to dry for approximately 48 h and then detached from the PVDF surface carefully from the edges using a knife.

The PVA film was cut into squares of size 10 cm × 10 cm, with a 1 cm × 1 cm grid drawn onto the film to track the uniformity of stretching. Finally, the film was heated to 130 °C and uniaxially stretched with a biaxial film stretcher to the desired elongation. Following stretching, sections of the film that stretched uniformly were cut and dissolved in a 3:7 solution of isopropyl alcohol (IPA) and ultra-pure water. Dissolution was conducted over 12 h. The suspensions of ellipsoids in dissolved PVA, IPA, and water was centrifuged and redispersed in a 3:7 solution of IPA andwater three times to remove PVA. Following these washing steps, the ellipsoids were further cleaned by centrifugation and re-dispersal in ultra-pure water seven times. The ellipsoids were finally dispersed in a KCl solution of a concentration of 10^{-4} M.

2.2. Assembly of fluid cell and experimental protocol

The experimental setup consisted of a parallel plate electrochemical fluid cell observed via a regular upright microscope. The cell was assembled by sandwiching fluid between two electrodes (see Fig. 1). The electrodes were two tin-doped indium oxide (ITO) coated glass slides (with a surface resistivity of 30–60 Ω/sq., purchased from Sigma Aldrich). Silver conductive epoxy adhesives were used to attach the conducting wire on the ITO sliders. The electrodes were first sonicated in acetone and IPA for 10 min., respectively, and then plasma cleaned for 2 min. Afterward, the electrodes were rinsed with ultra-pure water and soaked in a KCl and poly(sodium-p-styrenesulfonate) solution for another 15 min bath sonication. One 120 μm deep Secure-Seal™ (Invitrogen) was placed on the conducting side of one slide. Each of the eight wells in the space was filled with 10.5 μL of the suspended ellipsoids. The fluid cell was then sealed by placing a second ITO slide on top. The electric field was applied with a Reference 600+ Potentiostat/Galvanostat/ZRA (Gamry Instruments) implemented with the Virtual Panel user interface. The images were captured under a 20× objective (NA = 0.45, 511.9 nm/pixel) via a digital deep-cooled camera

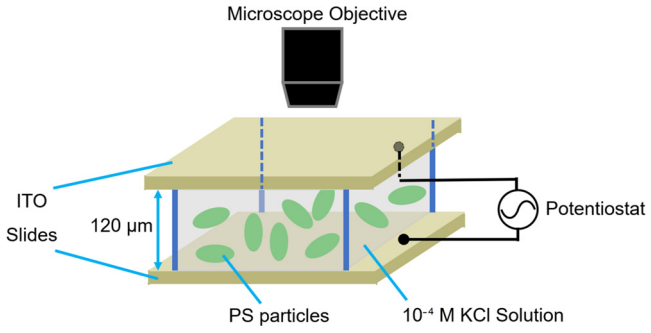

Fig. 1. Experimental setup for the response of colloidal particles to an *ac* electric field. Colloidal ellipsoids settle to the bottom electrode as a consequence of gravity. Strong negative equilibrium charges bound to both the particle and electrode contribute to the particles remaining mobile.

(Hamamatsu C10600). Experiments summarized herein were executed in potentiodynamic (potential controlled) mode at low frequencies. Experiments in which structure was measured kept the nominal potential drop fixed and ramped the frequency in steps spaced one minute apart. When measuring the rate constant associated with aggregation, no electric field was introduced for the first 15 s and then followed by applying an electric field of a fixed potential and frequency for another 45 s. A very similar protocol was previously employed for measuring the kinetics of aggregation for isotropic spheres [14]. As noted elsewhere [16], the electric field does not saturate until frequencies > 100 Hz when operating in potential controlled mode. Herein, we reported the nominal potential drop ($\Delta\Phi$) across the electrode separation distance.

2.3. Structure and rate constant analysis

Particles undergo a process of electric field mediated aggregation or separation that is somewhat different from other flocculation processes experienced by active colloidal suspensions. Herein, particles do not experience a dynamic assembly process in which clusters form and disintegrate for a given condition. Rather, particles tend to either aggregate or separate, depending on the electric field conditions. Thus, it is unnecessary to consider the process to form "living" clusters as has been done elsewhere [36]. Rather, we seek to track first whether particles will aggregate or separate at a given conditions and second with what rate constant the aggregation process occurs.

Digital video microscopy was used to capture the response of ellipsoids to the nearby polarized electrode. Images were captured at 8 frames per second (fps) with a 10 ms exposure time. The longest duration video was 17 min. In experiments where the ensemble structure was measured, there was no external electric field during the first and last minute, but once the electric field was introduced, the applied potential was fixed while the applied frequency was tuned every 1 min to ramp up from 25 Hz to 3000 Hz, and then ramp down to 25 Hz, which led to 17 conditions in total for a single video. Three potential drops were used when controlling potential (1.0 V, 1.5 V, and 2.0 V). Videos were saved as .avi files and were analyzed with Fiji (https://fiji.sc/).

Two quantities were measured and reported herein. First, the scaled mean cluster projected area was measured via the projected mean area of all objects in view (see Fig. 2(a) – (d)). The scaled cluster projected area D_c was defined as the quotient of the average dynamic D_t and average initial D_0 cluster projected area. Particles attracted to each other will result in an increase in D_c as a function of time (see Fig. 2(a) to (b) and Fig. 2(c) to (d)), while repelling particles will be measured to have a decrease in D_c as a function of time (see Fig. 2(b) to (c)).

Second, the rate constant for the aggregation of ellipsoids responding to an electric field was measured. As was done previously for spherical colloids responding to an electric field [14], the rate constant was equated with the short time loss of singlets in our experiments starting from monodisperse conditions. This treatment is appropriate for our experiments both because the short time loss of singlets dominates the aggregation process and there is no breakup of clusters once formed (i.e. there are no living clusters). Briefly, consider the ensemble of particles in a single plane shown in Fig. 2(e) – (h). These representative micrographs show only the remaining singlet ellipsoids as a function of time in response to an electric field. When only considering singlets assembling into doublets without cluster breakup, the singlet loss rate is given by:

$$\frac{dn_1}{dt} = -k_e n_1^2 \tag{1}$$

Where n_1 is the concentration of singlets, which equals to the number of singlets in the region of interest divided by the area of the region of interest and k_e is the rate constant in units of area/time. Following the integration of Eq. 1 and defining $n_1(t = 0) = n_{1,0}$ [14]:

$$\frac{n_{1,0}}{n_1} = 1 + k_e n_{1,0} t \tag{2}$$

Eq. 2 is of utility in the experiments described below where singlet concentration was directly measured. Rearranging Eq. 3 such that the product of k_e and t are isolated:

$$\frac{1}{n_1} - \frac{1}{n_{1,0}} = k_e t \tag{3}$$

Thus, plotting the left-hand side of Eq. 3 versus time should give a straight line with slope equal to the rate constant, k_e. Herein, we measured the slope over the first 15 s of the 45-second application of

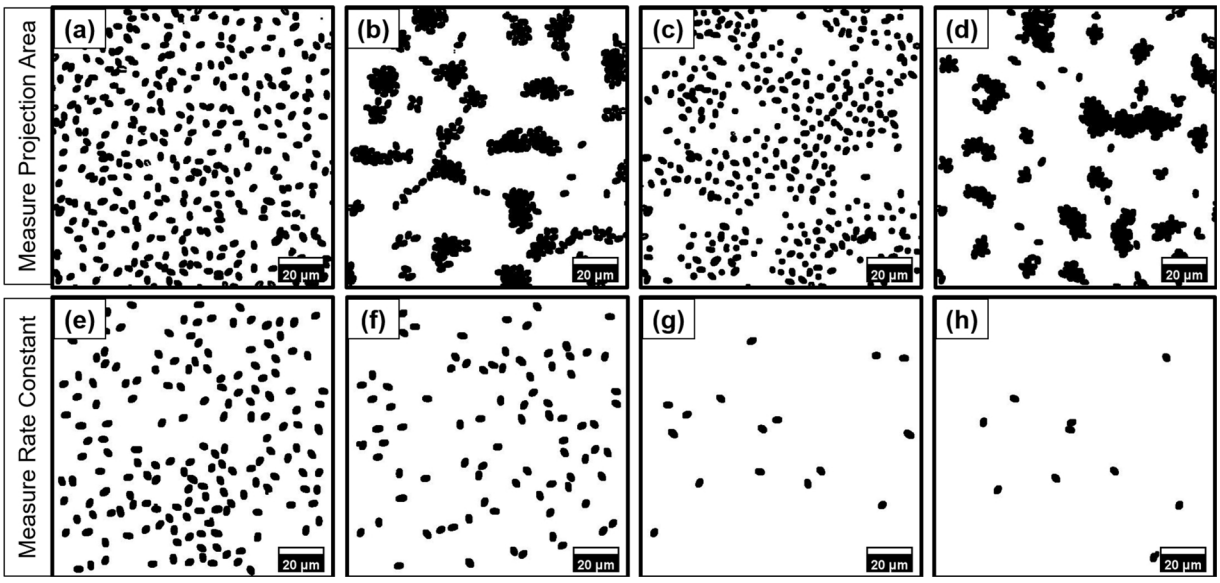

Fig. 2. Processed binary videos of colloidal particles in response to a nearby *ac* polarized electrode. Tracking the average cluster projected area and total area coverage over time to measure structure: (a) 0 min (no electric field), (b) 2 min (50 Hz, $\Delta\Phi$ = 2.0 V ramp up), (c) 10 min (500 Hz, $\Delta\Phi$ = 2.0 V, ramp down), (d) 14 min (50 Hz, $\Delta\Phi$ = 2.0, ramp down). Tracking the number of singlets over time to measure rate constant with electric field conditions of $\Delta\Phi$ = 2.0 and frequency = 50 Hz: (e) 0 s, (f) 20 s, (g) 40 s, (h) 60 s. Note that in (e) – (h) only the particles that remain singlets are shown, while all other objects in the frame have formed multibody clusters.

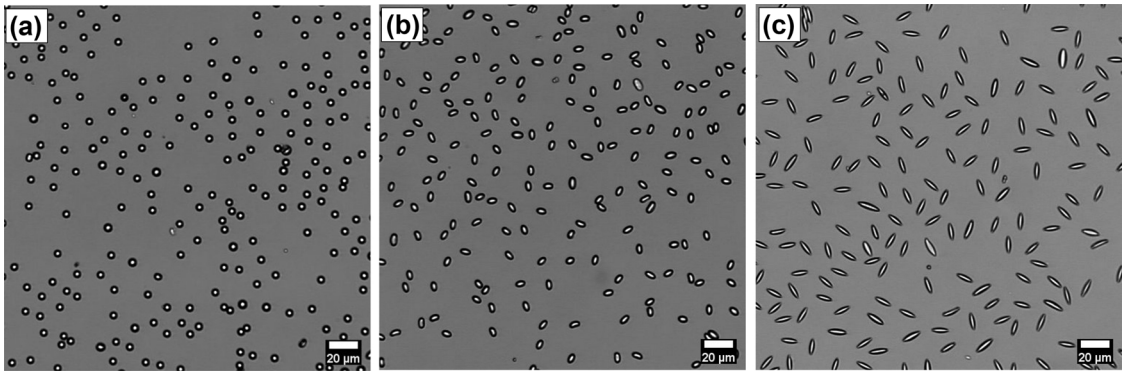

Fig. 3. Micrographs (500 × 500 pixels) of three particle samples (a) processed spheres, (b) low aspect ratio (LAR) ellipsoids, and (c) high aspect ratio (HAR) ellipsoids.

the electric field. The rate constant is expected to depend on the electric field conditions. A particle system aggregating strongly at a given set of electric field conditions will have a larger rate constant when compared to a system aggregating less strongly at a different set of conditions. Previous work has shown that spheres have a rate constant that depended on the square of the electric field strength and on the inverse of the frequency [14].

3. Results and discussion

3.1. Fabrication and characterization of colloidal ellipsoids

Fig. 3 shows optical micrographs of ellipsoids prepared via the film stretching technique described in the previous section, along with spheres that were processed in the same way as the ellipsoids, except without stretching. Two populations of ellipsoids were prepared for the experiments described herein. "Low aspect ratio (LAR)" ellipsoids had an aspect ratio of 1.39 ± 0.08 (see Fig. 3(b)), while "high aspect ratio (HAR)" ellipsoids had an aspect ratio of 2.30 ± 0.16 (see Fig. 3(c)). Ellipsoids were somewhat polydisperse as a consequence of a variety of factors. First, feedstock spheres had a nominal diameter of 5 μm, but were polydisperse. The polydispersity of native spheres translated to ellipsoid populations with polydisperse aspect ratio. Second, the macroscopic film stretch was non-uniform. This effect was mitigated by presorting populations of particles by processing films together that stretched similarly to each other. Finally, a more minor factor leading to non-uniformity in aspect ratio was that of particle location within the film. Particles located at or near the film-air interface did not stretch uniformly, however, this likely only impacts a small fraction of particles because there would be far more particles dispersed in the volume of the film than near or at the interface.

3.2. Ellipsoid response to electric field

Initially, the average cluster projected area and total area coverage were tracked for ensembles of colloidal spheres and ellipsoids of varying aspect ratio in response to an electric field of varying strength and frequency. The scaled cluster projected area was measured to determine whether particles aggregated or separated (or neither) at a given electric field condition. The slope of the dynamic cluster projected area at a given electric field and frequency conditions $\frac{dD_c}{dt}_{E_0,f}$ is an indicator of this behavior, which results from the net electrokinetic mediated hydrodynamic force felt by individual particles in the ensemble.

Specifically, electrokinetic flows originate from action of electric field components on mobile charge accumulated near either the particle or electrode. Induced-charge electroosmosis (ICEO) and equilibrium-charge electroosmosis (ECEO) are two electrokinetic flows that have been shown to induce either aggregation or separation among colloidal particles in response to an electric field [4]. For ICEO, polarization induces the accumulation of excess surface charge on the electrode. The nearby particle causes electric field components to be tangent to the electrode that acts on the induced mobile charge associated with the electrode to produce ICEO flow. Further, ECEO flow arises when the electric field acts on the equilibrium charge associate with the diffuse layer of a particle. Both ICEO and ECEO flow generate toroidal flow with a direction that depends on a variety of factors, including electric field and solution conditions. When the combination of these flows pump towards and upward along the particle, neighboring particles will aggregate. However, neighboring particles will separate when these flows combine to pump downward along the particle and outward.

We chose to begin with spheres processed in the same way as ellipsoids to isolate the impact of shape (rather than processing) on the response of particles to an electric field. These control experiments were conducted to determine whether dispersing polystyrene colloids in PVA had any significant impact on the response of these particles to electric fields. Increasing (decreasing) average cluster projected area is indicated by a region with a positive (negative) slope, showing aggregation (separation) (see Fig. 4). The particles experienced aggregation when $\frac{D_t}{D_0} > 1$ and $\frac{dD_c}{dt}_{E_0,f} \geq 0$, and experienced separation when $\frac{D_t}{D_0} = 1$ or $\frac{dD_c}{dt}_{E_0,f} < 0$.

Processed spherical colloids had regions of aggregation and separation depending on the electric field frequency and strength (see Fig. 4(a)). Spherical particles tended to aggregate strongly at low frequency. Further, increasing the electric field strength tended to boost the magnitude of the response rate of particles aggregation. However, increasing the electric field strength did not induce a strong increase in the response rate of particles separation. Finally, note from Fig. 4 how ensemble behavior for aggregating conditions depended on electric field strength. There was a shift in the critical frequency experienced by the spherical particles. As the electric field frequency approached 200 Hz, aggregation plateaued, crossed a critical frequency, and then particles began to separate at frequencies greater than or equal to 300 Hz when the electric field strength set as 1.0 V or 1.5 V. However, for 2.0 V at 300 Hz, the aggregation reached another plateau, which is lower than the previous one, suggesting the critical frequency would increase as the applied electric field strength increases. These data were used to formulate a structure diagram (see Fig. 4(b)). The main features of the structure diagram for spheres are the shifted presence of a critical frequency f_c (200 Hz–300 Hz for 1.0 V, 1.5 V, and 300 Hz–500 Hz for 2.0 V) regardless of the ramp of tuning frequency.

Low aspect ratio (LAR) ellipsoids displayed behavior different from that of spheres. LAR ellipsoids rapidly aggregated at low frequency, reached a critical frequency $f_c \sim$ 300 Hz–500 Hz, and then began to separate at frequencies between ≥ 500 Hz (see Fig. 5(a)). One feature that was unique to LAR ellipsoids was the reorientation in the axis

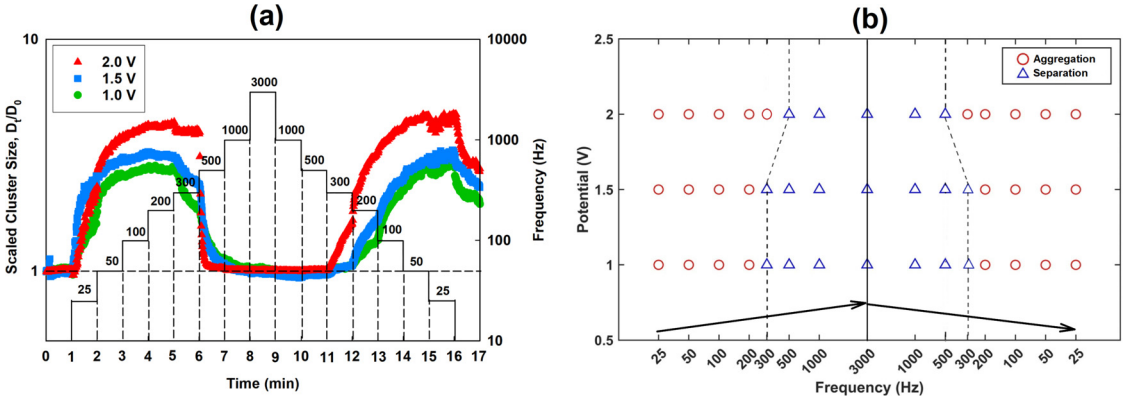

Fig. 4. Dynamic structural evolution of colloidal spheres in response to a nearby *ac* polarized electrode. (a) Coloring of each data point indicates electric field strength and the inset numbers from 25 Hz – 3000 Hz indicate the frequency applied over that time period. Spherical colloidal particles processed in the same way as ellipsoids (without stretching) experienced shifted regimes of aggregation and separation, depending on field strength. In particular, spheres aggregated at all electric field strengths and increasing frequencies ≤ 200 Hz and repelled at all frequencies ≥ 500 Hz. However, at frequencies 300 Hz - 500 Hz, spherical colloids at 1.0 V and 1.5 V responded differently from spherical colloids at 2.0 V. (b) Structure diagram assembled from the data summarized in (a). Regions with a non-negative slope and $\frac{D_t}{D_0} > 1$ in (a) were considered regions of 'aggregation', while regions with either a negative slope or $\frac{D_t}{D_0} = 1$ in (b) were considered to be regions of 'separation'. The solid line indicates where the frequency ramp reversed and the broken lines indicate where particles response changed.

parallel to the electrode at certain frequencies. Evidence of ellipsoids reorienting such that the long axis was perpendicular to the electrode (standing ellipsoid) was first seen in the average cluster projected area measurement (see Fig. 5(a)). Standing is apparent when the scaled average cluster projected area decreased below the reference line ($D_c/D_0 < 1$) at times between 8 min – 10 min. The scaled average cluster projected area decreased due to a decrease in the projected area of the ellipsoid. A standing ellipsoid will have a circular projected area, as compared to a laying ellipsoids with an elliptical projected area. Similar to spheres, these data were used to formulate a structure diagram (see Fig. 5(b)). Note the asymmetry of the ensemble behavior for aggregating conditions. There was a hysteresis in the critical frequency experienced by LAR ellipsoids: the presence of a critical frequency $f_c \sim$ 300 Hz–500 Hz for all electric field strengths when increasing the frequency, but a critical frequency $f_c \sim$ 1000 Hz - 500 Hz when decreasing frequency.

The structure diagram in Fig. 5(b) has features that are unique when compared to the structure diagram for spheres. First, besides the hysteretic behavior, the LAR ellipsoids have a constant and larger critical frequency as compared to that of spheres. LAR ellipsoids experience the separation at increasing frequencies ≥ 500 Hz and decreasing frequencies ≥ 1000 Hz. Second, LAR ellipsoids also displayed hysteresis in the frequencies over which LAR ellipsoids align parallel with the electric field. Ellipsoids aligned at a frequency of 3000 Hz when ramping up in frequency, but did not relax to an orientation roughly perpendicular to the electric field until a frequency of ~500 Hz when ramping down in frequency. This behavior is a consequence of the balance between stochastic Brownian rotation, hindered rotational mobility, and electric field mediated dipole torque. An ellipsoid will stand when ramping frequency at the condition where the electric field induced dipole moment is sufficient to overcome rotational hindrance from the nearby boundary and stochastic fluctuations away from an orientated state. When ramping down in frequency and decreasing dipole torque, the balance of these effects produce a finite relaxation time for the ellipsoid to reorient such that the long axis is parallel to the electrode surface. Given the unhindered rotational diffusion time for spherical particles of this volume is ~27 s, with the hindered rotational diffusion time longer depending on the most probable separation distance of the particle, we expect such relaxation to be observable and potentially longer than the electric field stepping conditions. Thus, the hysteresis observed in

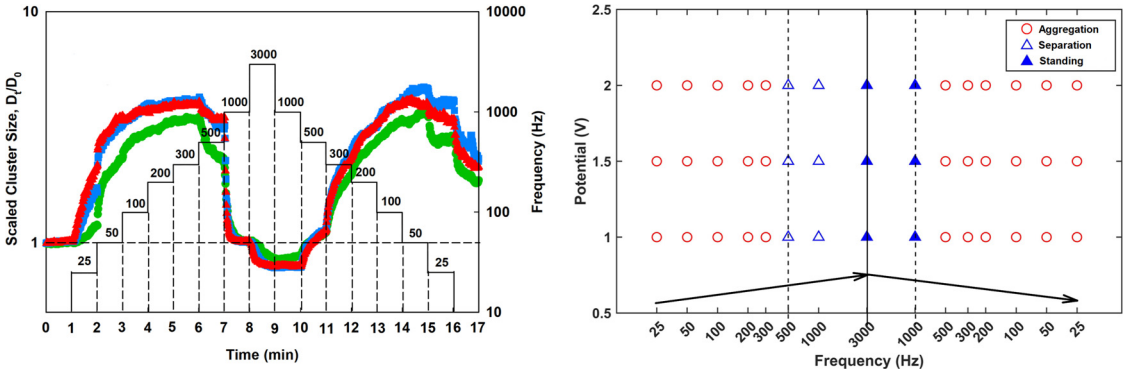

Fig. 5. Dynamic structural evolution of low aspect ratio (LAR) ellipsoids in response to a nearby *ac* polarized electrode. (a) Coloring of each data point indicates electric field strength and the inset numbers from 25 Hz – 3000 Hz indicate the frequency applied over that time period. Unlike spherical colloidal particles, LAR experienced hysteretic regimes of aggregation and separation. In particular, LAR ellipsoids aggregated at all electric field strengths and increasing frequencies roughly ≤ 300 Hz and separated from each other at increasing frequencies ≥ 500 Hz. Yet, LAR ellipsoids experienced the separation at all electric strengths and decreasing frequencies ≤ 1000 Hz. In addition, LAR ellipsoids aligned with the direction of the electric field (i.e. standing) at the envelope of frequencies with an upper bound of 3000 Hz and decreasing frequency 1000 Hz. (b) Structure diagram assembled from the data summarized in (a). Regions with a non-negative slope and $\frac{D_t}{D_0} > 1$ in (a) were considered regions of 'aggregation', while regions with a negative slope or $\frac{D_t}{D_0} = 1$ in (b) were considered regions of 'separation'. The solid line indicates where the frequency ramp reversed and the broken lines indicate where particles response changed.

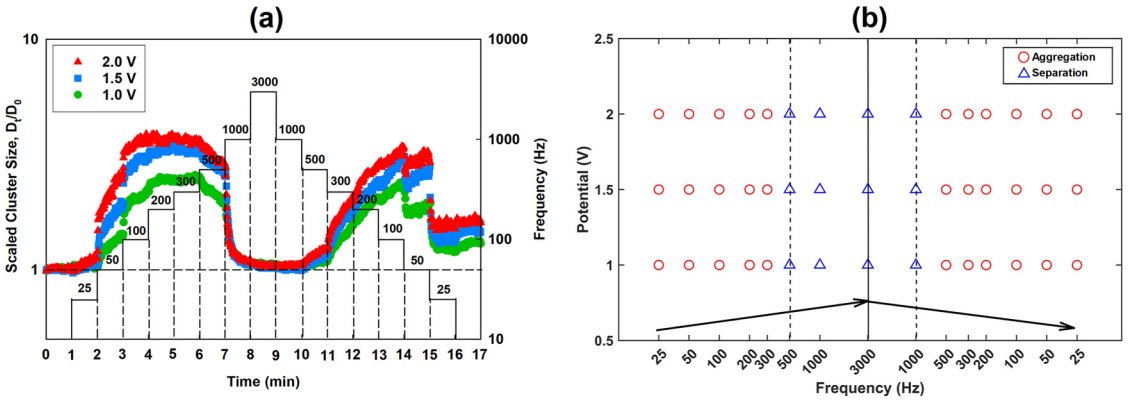

Fig. 6. Dynamic structural evolution of high aspect ratio (HAR) ellipsoids in response to a nearby *ac* polarized electrode. **(a)** Coloring of each data point indicates electric field strength and the inset numbers from 25 Hz – 3000 Hz indicate the frequency applied over that time period. Similar to LAR ellipsoids, HAR experienced hysteretic regimes of aggregation and separation. HAR ellipsoids aggregated at all electric field strengths and increasing frequencies roughly ≤ 300 Hz and separated at increasing frequencies ≥ 500 Hz. Further, HAR ellipsoids experienced the aggregation at all electric strengths and decreasing frequencies ≤ 1000 Hz. However, unlike LAR ellipsoids, there were no regimes in which HAR ellipsoids were observed to align with the direction of the electric field (i.e. standing). **(b)** Structure diagram assembled from the data summarized in (a). Regions with a non-negative slope and $\frac{D_f}{D_0} > 1$ in (a) were considered regions of 'aggregation', while regions with either a negative slope or $\frac{D_f}{D_0} = 1$ in (b) were considered regions of 'separation'. The solid line indicates where the frequency ramp reversed and the broken lines indicate where particles response changed.

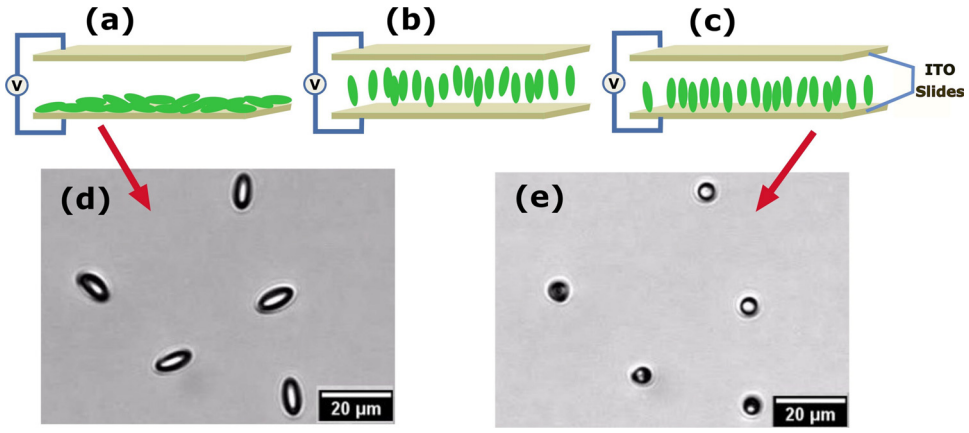

Fig. 7. Schematic of protocol to deposit LAR ellipsoids in a standing orientation. (a) Prior to application of an electric field, ellipsoids experiencing Brownian fluctuations with the long axis orientated roughly parallel to the electrode. (b) Ellipsoids align the long axis in the direction of the nominal electric field at conditions summarized in Fig. 5. (c) A pulse of a *dc* electric field will deposit the LAR ellipsoids at an orientation nearly perpendicular to the electrode substrate. The deposited ellipsoids are long-lasting while in liquid. (d) Image of a group of ellipsoid particles before applying electric field. (e) Stuck particles after applying *ac* and *dc* field.

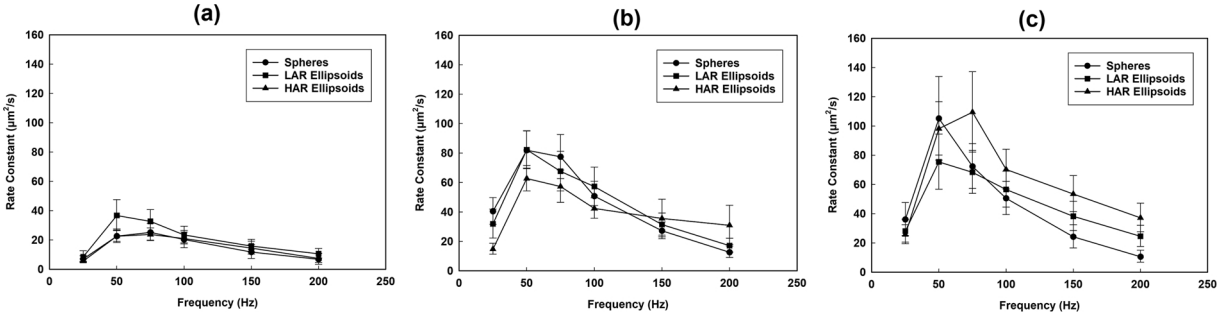

Fig. 8. Rate constants for aggregation of processed spheres, LAR ellipsoids, and HAR ellipsoids. The rate constant was measured for a range of frequencies and varying electric field strength, including (a) 1.0 V, (b) 1.5 V, and (c) 2.0 V. All systems responded in qualitatively the same way. The rate constant for aggregation grew as frequency increased from 25 Hz, reached a maximum, and then started to decrease as frequency was increased to regions where particles began to experience the separation. Although the qualitative behavior was the same, the magnitude of the rate constant increased as a function of the nominal electric field strength. These data suggest there is no strong dependence of particle shape on the aggregation rate constant at these conditions. Each rate constant reported herein is the mean value of six separate experiments and the error bars represent the standard error of the mean.

standing in these data is likely a partial consequence of the rotational diffusion time for the particles being similar to that of the electric field time step.

High aspect ratio (HAR) ellipsoids experienced trends in the response to the nearby electrode similar to that of LAR ellipsoids (see Fig. 6). HAR ellipsoids aggregated for all electric field strengths up to a critical frequency of ~300 Hz and separated for frequencies between 500 Hz – 3000 Hz. The primary difference between LAR and HAR ellipsoids was in the presence of a standing state. HAR ellipsoids did not align for any of the conditions tested herein. This supports the hypothesis that the hysteresis is a consequence of the balance between rotational relaxation and hindered mobility. Although one would

expect the induced dipole torque experienced by HAR and LAR ellipsoids to be approximately the same at these conditions [37], hindered rotational mobility will differ. A LAR ellipsoid will have a larger rotational mobility about the polar angle as compared to a HAR as a consequence of hindrance induced by the nearby boundary. Apparently, the induced dipole torque was insufficient to overcome hindered rotational mobility to align the HAR ellipsoid in the direction of the electric field at these conditions.

3.3. Deposition of standing ellipsoids

Alignment of the LAR ellipsoids in the direction of the electric field could potentially be utilized for fixing ellipsoidal particles at orientations that typically would be energetically inaccessible in the absence of an *ac* electric field. Prior to application of the oscillatory electric field, ellipsoidal particles are at orientations such that the long axis of the particle is roughly parallel to the substrate (see Fig. 7(a) and (d)). Initially, an electric field is applied at conditions expected to induce standing (see Fig. 7(b)). After a sufficient number of ellipsoids align with the electric field, application of a *dc* electric field > 2 V induces sticking (see Fig. 7(c) and (e)) (see SI for videos demonstrating particle relaxation and sticking). Previous work has demonstrated that spherical particles can be made to stick upon application of a steady electric field [38]. A steady *dc* electric field will produce a steady electrophoretic force on the ellipsoidal particle in either the direction of the nearby electrode or to the other side of the fluid cell [39,40]. Ultimately, the steady force needs to overcome the potentially strong electrostatic repulsion that will arise from the equilibrium charge bound to both the electrode substrate and particle. Immediate application of the *dc* field while the *ac* field is on will induce sticking of ellipsoids in an orientation nearly perpendicular to the substrate because the ellipsoid does not have sufficient time to relax. Waiting a finite amount of time between switching of the fields allows for the ellipsoid to relax to orientations intermediate between perpendicular and parallel to the electrode substrate.

3.4. Kinetics of aggregation for spheroidal colloids

Data summarized above provided a semi-quantitative description of the response of spheroids with varying aspect ratio to a nearby polarized electrode. We obtained a quantitative description of aggregation kinetics by treating the process with the framework of a chemical reaction. The primary feature of such a treatment is measuring a rate constant associated with singlet loss (see Section 2.3 for the description). This treatment was previously used for spheres; we repeat similar measurements with processed spheres and extend the measurements to ellipsoids. Our primary motivation is to determine whether there was an impact of aspect ratio on the rate constant for aggregation in response to an *ac* electric field. Initially, the rate constant for processed spheres was measured at systemically different frequencies and varying nominal electric field. These measurements were followed-up by experiments on LAR and HAR ellipsoids. Fig. 8 shows a summary of the rate constant for all systems at varying frequency at different fixed electrode polarization.

Processed spheres, LAR ellipsoids, and HAR ellipsoids all had rate constants for aggregation that were qualitatively similar. The rate constant for each system increased from 25 Hz with frequency at fixed nominal electric field, reaching a maximum between 50 Hz – 100 Hz. Once the frequency was increased beyond this maximum, the rate constant decreased monotonically with frequency until reaching the critical frequency identified for each system in Section 3.2. Note the range of rate constants measured herein for processed spheres matched that of the range measured previously [14], which indicates the film casting process does not have a significant impact on the response of these particles to a nearby electrode. There was no apparent difference in rate constant between systems of different aspect ratios for fixed nominal electric field. However, the magnitude of the rate constant did increase monotonically for increases in the nominal electric field strength. Although LAR and HAR ellipsoids experience slight differences in the structural response to an electric field when compared to spheres, the rate constant with which these systems aggregate does not strongly depend on aspect ratio.

4. Conclusions

Colloidal particles with anisotropic shape or chemistry have the potential to be used as building blocks for complex structures. Utilization of an external electrical field is one strategy for assembling these particles into complex structures. Herein, we conducted structure and kinetic rate experiments to quantify the response of ellipsoidal particles to a nearby electrode polarized with a low-frequency *ac* electric field. Ellipsoidal particles displayed a qualitatively different response depending on the aspect ratio. While both displayed a hysteretic behavior in aggregation and separation, with regimes of frequency matching each type of interaction, only the low aspect ratio ellipsoids aligned with the direction of the electric field at some conditions. Further, additional measurements probing the aggregation rate of ellipsoids in response to an *ac* electric field showed the same qualitative behavior, regardless of aspect ratio. An additional set of experiments utilizing this information was conducted to show that long-lasting deposition of ellipsoids in energetically unfavorable orientations could be achieved. Such structures could be useful as model systems for light scattering problems or more generally useful for building complex structures. Together, experiments and data summarized herein illustrate that although there are some specific qualitative differences in the response of spheroids to an electric field as a consequence of aspect ratio, the general behavior is very similar at these aspect ratios. Consequently, previous work on spheres is likely applicable to ellipsoids of these aspect ratios.

Author contributions

The manuscript was written through contributions of all authors. All authors have given approval to the final version of the manuscript.

All authors contributed equally to the manuscript.

Declaration of Competing Interest

The authors declare that they have no known competing financial interests or personal relationships that could have appeared to influence the work reported in this paper.

Acknowledgements

This work was supported by the Cleveland State University Office of Research Startup Fund and Faculty Research Development Grant, and the National Science Foundation CAREER Award, NSF no. 1752051.

Appendix A. Supplementary data

Supplementary material related to this article can be found, in the online version, at doi:https://doi.org/10.1016/j.colsurfa.2020.125384.

References

[1] S.O. Lumsdon, E.W. Kaler, O.D. Velev, Two-dimensional crystallization of microspheres by a coplanar AC electric field, Langmuir 20 (2004) 2108–2116, https://doi.org/10.1021/la035812y.

[2] J.D. Forster, J.G. Park, M. Mittal, H. Noh, C.F. Schreck, C.S. O'Hern, H. Cao, E.M. Furst, E.R. Dufresne, Assembly of optical-scale dumbbells into dense photonic crystals, ACS Nano 5 (2011) 6695–6700, https://doi.org/10.1021/nn202227f.

[3] F. Li, D.P. Josephson, A. Stein, Colloidal assembly: the road from particles to colloidal molecules and crystals, Angew. Chem. Int. Ed. Engl. 50 (2011) 360–388,

https://doi.org/10.1002/anie.201001451.
[4] D.C. Prieve, P.J. Sides, C.L. Wirth, 2-D assembly of colloidal particles on a planar electrode, Curr. Opin. Colloid Interface Sci. 15 (2010) 160–174, https://doi.org/10.1016/j.cocis.2010.01.005.
[5] J.A. Fagan, P.J. Sides, D.C. Prieve, Mechanism of rectified lateral motion of particles near electrodes in alternating electric fields below 1 kHz, Langmuir 22 (2006) 9846–9852, https://doi.org/10.1021/la060899j.
[6] J.D. Hoggard, P.J. Sides, D.C. Prieve, Electrolyte-dependent pairwise particle motion near electrodes at frequencies below 1 kHz, Langmuir 23 (2007) 6983–6990, https://doi.org/10.1021/la070049j.
[7] C.L. Wirth, R.M. Rock, P.J. Sides, D.C. Prieve, Single and pairwise motion of particles near an ideally polarizable electrode, Langmuir 27 (2011) 9781–9791, https://doi.org/10.1021/la2017038.
[8] Y. Liu, X.-Y. Liu, J. Narayanan, Kinetics and equilibrium distribution of colloidal assembly under an alternating electric field and correlation to degree of perfection of colloidal crystals, J. Phys. Chem. C 111 (2007) 995–998, https://doi.org/10.1021/jp0657282.
[9] C.S. Dutcher, T.J. Woehl, N.H. Talken, W.D. Ristenpart, Hexatic-to-disorder transition in colloidal crystals near electrodes: rapid annealing of polycrystalline domains, Phys. Rev. Lett. 111 (2013) 128302, https://doi.org/10.1103/PhysRevLett.111.128302.
[10] T.J. Woehl, K.L. Heatley, C.S. Dutcher, N.H. Talken, W.D. Ristenpart, Electrolyte-dependent aggregation of colloidal particles near electrodes in oscillatory electric fields, Langmuir 30 (2014) 4887–4894, https://doi.org/10.1021/la4048243.
[11] S. Saini, S.C. Bukosky, W.D. Ristenpart, Influence of electrolyte concentration on the aggregation of colloidal particles near electrodes in oscillatory fields, Langmuir 32 (2016) 4210–4216, https://doi.org/10.1021/acs.langmuir.5b04636.
[12] J. Kim, S.A. Guelcher, S. Garoff, J.L. Anderson, Two-particle dynamics on an electrode in ac electric fields, Adv. Colloid Interface Sci. 96 (2002) 131–142, https://doi.org/10.1016/S0001-8686(01)00078-1.
[13] Y. Solomentsev, M. Böhmer, J.L. Anderson, Particle clustering and pattern formation during electrophoretic deposition: a hydrodynamic model, Langmuir 13 (1997) 6058–6068, https://doi.org/10.1021/la970294a.
[14] W.D. Ristenpart, I.A. Aksay, D.A. Saville, Assembly of colloidal aggregates by electrohydrodynamic flow: kinetic experiments and scaling analysis, Phys. Rev. E 69 (2004) 021405, , https://doi.org/10.1103/PhysRevE.69.021405.
[15] W.D. Ristenpart, I.A. Aksay, D.A. Saville, Electrohydrodynamic flow around a colloidal particle near an electrode with an oscillating potential, J. Fluid Mech. 575 (2007) 83, https://doi.org/10.1017/S0022112006004368.
[16] C.L. Wirth, P.J. Sides, D.C. Prieve, Electrolyte dependence of particle motion near an electrode during ac polarization, Phys. Rev. E 87 (2013) 032302, , https://doi.org/10.1103/PhysRevE.87.032302.
[17] J.A. Fagan, P.J. Sides, D.C. Prieve, Evidence of multiple electrohydrodynamic forces acting on a colloidal particle near an electrode due to an alternating current electric field, Langmuir 21 (2005) 1784–1794, https://doi.org/10.1021/la048076m.
[18] J.A. Fagan, P.J. Sides, D.C. Prieve, Calculation of ac electric field effects on the average height of a charged colloid: effects of electrophoretic and Brownian motions, Langmuir 19 (2003) 6627–6632, https://doi.org/10.1021/la0340706.
[19] J.A. Fagan, P.J. Sides, D.C. Prieve, Vertical oscillatory motion of a single colloidal particle adjacent to an electrode in an ac electric field, Langmuir 18 (2002) 7810–7820, https://doi.org/10.1021/la025721l.
[20] J.A. Fagan, P.J. Sides, D.C. Prieve, Vertical motion of a charged colloidal particle near an AC polarized electrode with a nonuniform potential distribution: theory and experimental evidence, Langmuir 20 (2004) 4823–4834, https://doi.org/10.1021/la036022r.
[21] K.L. Heatley, F. Ma, N. Wu, Colloidal molecules assembled from binary spheres under an AC electric field, Soft Matter 13 (2017) 436–444, https://doi.org/10.1039/C6SM02091G.
[22] F. Ma, D.T. Wu, N. Wu, Formation of colloidal molecules induced by alternating-current electric fields, J. Am. Chem. Soc. 135 (2013) 7839–7842, https://doi.org/10.1021/ja403172p.
[23] F. Ma, S. Wang, L. Smith, N. Wu, Two-dimensional assembly of symmetric colloidal dimers under electric fields, Adv. Funct. Mater. 22 (2012) 4334–4343, https://doi.org/10.1002/adfm.201200649.
[24] F. Ma, S. Wang, H. Zhao, D.T. Wu, N. Wu, Colloidal structures of asymmetric dimers via orientation-dependent interactions, Soft Matter 10 (2014) 8349–8357, https://doi.org/10.1039/c4sm01492h.
[25] F. Ma, S. Wang, D.T. Wu, N. Wu, Electric-field–induced assembly and propulsion of chiral colloidal clusters, Proc. Natl. Acad. Sci. 112 (2015) 6307–6312, https://doi.org/10.1073/pnas.1502141112.
[26] C.L. Wirth, S.H. Nuthalapati, Response of a doublet to a nearby dc electrode of uniform potential, Phys. Rev. E 94 (2016) 042614, , https://doi.org/10.1103/PhysRevE.94.042614.
[27] S. Gangwal, A. Pawar, I. Kretzschmar, O.D. Velev, Programmed assembly of metallodielectric patchy particles in external AC electric fields, Soft Matter 6 (2010) 1413, https://doi.org/10.1039/b925713f.
[28] J.P. Singh, P.P. Lele, F. Nettesheim, N.J. Wagner, E.M. Furst, One- and two-dimensional assembly of colloidal ellipsoids in ac electric fields, Phys. Rev. E 79 (2009) 050401, , https://doi.org/10.1103/PhysRevE.79.050401.
[29] S. Hernández-Navarro, J. Ignés-Mullol, F. Sagués, P. Tierno, Role of anisotropy in electrodynamically induced colloidal aggregates, Langmuir 28 (2012) 5981–5986, https://doi.org/10.1021/la3002493.
[30] W. Xu, Z. Li, Y. Yin, Colloidal assembly approaches to micro/nanostructures of complex morphologies, Small 14 (2018), https://doi.org/10.1002/smll.201801083 1801083.
[31] S. Gangwal, O.J. Cayre, M.Z. Bazant, O.D. Velev, Induced-charge electrophoresis of metallodielectric particles, Phys. Rev. Lett. 100 (2008) 058302, , https://doi.org/10.1103/PhysRevLett.100.058302.
[32] J.G. Lee, A.M. Brooks, W.A. Shelton, K.J.M. Bishop, B. Bharti, Directed propulsion of spherical particles along three dimensional helical trajectories, Nat. Commun. 10 (2019) 2575, https://doi.org/10.1038/s41467-019-10579-1.
[33] C.W. Shields, K. Han, F. Ma, T. Miloh, G. Yossifon, O.D. Velev, Supercolloidal spinners: complex active particles for electrically powered and switchable rotation, Adv. Funct. Mater. 28 (2018), https://doi.org/10.1002/adfm.201803465 1803465.
[34] A. Doicu, A.A. Vasilyeva, D.S. Efremenko, C.L. Wirth, T. Wriedt, A light scattering model for total internal reflection microscopy of geometrically anisotropic particles, J. Mod. Opt. 66 (2019) 1139–1151, https://doi.org/10.1080/09500340.2019.1605005.
[35] C.C. Ho, A. Keller, J.A. Odell, R.H. Ottewill, Preparation of monodisperse ellipsoidal polystyrene particles, Colloid Polym. Sci. 271 (1993) 469–479, https://doi.org/10.1007/BF00657391.
[36] J. Palacci, S. Sacanna, A.P. Steinberg, D.J. Pine, P.M. Chaikin, Living crystals of light-activated colloidal surfers, Science (80-.) 339 (2013) 936–940, https://doi.org/10.1126/science.1230020.
[37] T.B. Jones, Electromechanics of Particles, Cambridge University Press, 2005.
[38] J. Gong, N. Wu, Electric-field assisted assembly of colloidal particles into ordered nonclose-packed arrays, Langmuir 33 (2017) 5769–5776, https://doi.org/10.1021/acs.langmuir.7b00547.
[39] C.L. Wirth, P.J. Sides, D.C. Prieve, The imaging ammeter, J. Colloid Interface Sci. 357 (2011) 1–12, https://doi.org/10.1016/j.jcis.2011.01.025.
[40] R.M. Rock, P.J. Sides, D.C. Prieve, The effect of electrode kinetics on electrophoretic forces, J. Colloid Interface Sci. 393 (2013) 306–313, https://doi.org/10.1016/j.jcis.2012.10.066.